Use of Wavelet Transforms in Segmentation of Retinal Angiography Images

DEBBOU Hanane

Laboratory of Electronics and New Technologies

Deoartement of Electrical Engineering University of Oum El Bouaghi, Algéria

debbou.hanane@univ-oeb.dz
debhanane@hotmail.com

MEGRI Abederrahim Fayçal

Laboratory of Electronics and New Technologies

Department of Electrical Engineering University of Oum Elbouaghi, Algeria

f.megri@univ-oeb.dz
f_megri@yahoo.fr

GHENNAM Souhaila

Laboratory of signal processing

Department of Electrical Engineering University of Bejaia, Algeria

Souhaila.ghennam@univ-bejaia.dz
ghsouhi@yahoo.fr

Abstract

Medical imaging plays a very important role in the non-invasive visualization of anatomical components in humans. In this work we focus on the retinal fundus by studying retinal angiography images. An algorithm for the extraction of the vascular tree has been developed, based on the enhancement by means of the Shrearlet transform, then on the decomposition by the continuous wavelet transform via the Morlet wavelet to finally proceed to a segmentation based on the thresholding on histogram.

I. Introduction

The rapid development of medical imaging technologies is revolutionizing medicine. Medical imaging provides scientists and physicians with vital information about the human body and is playing an increasingly important role in the diagnosis and treatment of diseases. Among the medical imaging, we count the retinal imaging which today is more and more concerted to diagnose pathologies affecting the retina and other diseases. The objective of our work is to detect the retinal vascular tree from a retinal angiography image and to extract it by segmentation, in order to eventually provide diagnostic assistance. Given the variability in terms of size, intensity and orientation of retinal vessels, we plan to approach this extraction via wavelet transformation, as it is a multi-resolution approach, which will allow us to explore the vessels under different scales. We will adopt the classical wavelet transform in its different aspects, as well as another variant which is the Shearlet transform.

II. The wavelet transform

The wavelet transform, which appeared at the beginning of the 80's [1], is a signal processing tool allowing the analysis of local properties of complex signals on several time (or space) scales. Indeed, and as in the present work, the objective is to segment retinal vessels of various sizes (large or fine), in this case, under different scales, the wavelet transform could be well suited to this task.

A. *The wavelet*

A wavelet is an oscillating function (which explains the word 'wave') of zero mean, often noted $\psi(t)$, possessing a certain degree of regularity and whose support is finite (hence the name 'wavelet') [2]. The fact that the support is finite, we say that the wavelet is localized.

From this single function $\psi(t)$which is called the mother wavelet, we construct by translation of b and dilation of a a family of functions $\psi_{a,b}(t)$ which are the basic atoms:

$$\left\{\boldsymbol{\psi_{a,b}(t)} = \frac{\mathbf{1}}{\sqrt{\boldsymbol{a}}}\boldsymbol{\psi}\left(\frac{\boldsymbol{t-b}}{\boldsymbol{a}}\right)\right\}_{(\boldsymbol{a},\boldsymbol{b})\in \boldsymbol{R_0^+}\times \boldsymbol{R}} \qquad (1)$$

B. *2D Discrete Wavelet Transform*

In The Discrete Wavelet Transform (DWT) the translation parameters b and dilation a of the wavelet will be discretized as follows: $a = 2^j, b = k2^j$ for $(j,k) \in Z^2$. And from now on we will place a function, called the scale function noted φ which is to local approximations; it is associated with ψ which is to details. [3].

We then define the basic atoms of the wavelets, as well as the basic atoms of the scaling function:

$$\boldsymbol{\psi_{j,k}(t)} = \mathbf{2}^{\frac{-j}{2}}\boldsymbol{\psi}\left(\mathbf{2}^{-j}\boldsymbol{t}-\boldsymbol{k}\right), \quad \boldsymbol{for} \quad (\boldsymbol{j},\boldsymbol{k}) \in \boldsymbol{Z^2} \ (2)$$

$$\boldsymbol{\varphi_{j,k}(t)} = \mathbf{2}^{\frac{-j}{2}}\boldsymbol{\varphi}\left(\mathbf{2}^{-j}\boldsymbol{t}-\boldsymbol{k}\right), \quad \boldsymbol{for} \quad (\boldsymbol{j},\boldsymbol{k}) \in \boldsymbol{Z^2} \qquad (3)$$

Thus the computation of the coefficients of the approximation $\boldsymbol{\beta_{j,k}}$ and the details $\boldsymbol{\alpha_{j,k}}$ at a resolution j and translated from k, is done by :

$$\boldsymbol{\alpha_{j,k}} = \int_{-\infty}^{+\infty} \boldsymbol{s(t)}\,\boldsymbol{\psi_{j,k}(t)dt} \qquad (4)$$

$$\boldsymbol{\beta_{j,k}} = \int_{-\infty}^{+\infty} \boldsymbol{s(t)}\,\boldsymbol{\varphi}_{\boldsymbol{j,k}}\boldsymbol{(t)dt} \qquad (5)$$

And at reconstruction, the signal s(t) is restored from the approximation A_J at the last resolution J and the detail set D_j at all resolutions $j \leq J$ as follows:

$$\mathbf{s(t)} = \boldsymbol{A_J} + \sum_{\boldsymbol{j\leq J}} \boldsymbol{D_j} \qquad (6)$$

Where $A_j = \sum_{k\in Z} \beta_{j,k}\, \varphi_{j,k}(t)$
And $D_j = \sum_{k\in Z} \alpha_{j,k}\, \psi_{j,k}(t)$.

1. Implementation of the DWT-2D

There are mainly two fast decomposition-reconstruction algorithms for the discrete wavelets transform 2D DWT:

- Mallat algorithm: DWT with decimation
- Hole Algorithm: DWT without decimation

Both use appropriate filters to obtain the approximation coefficients and the detail coefficients in the three orientations (vertical, diagonal and horizontal). These filters are computed from the wavelet function and its associated scale function.

2. Decomposition filters:

For a wavelet ψ, the associated scaling function φ satisfies a fundamental relationship which is the following equation:

$$\frac{1}{2}\varphi\left(\frac{1}{2}\right) = \sum_{n\in Z} a_n\, \varphi(t-n) \qquad (7)$$

Due to the fact that φ is compactly supported, the sequence $(a_n)_{n\in Z}$ would therefore be of finite number and could be viewed as the coefficients of a finite impulse response (FIR) low-pass filter ω .

From this ω filter, four FIR filters are defined [3]:

2 for the decomposition:

- LoD low-pass filter, to calculate the coefficients of the approximation $\beta_{j,k}$
- HiD high-pass filter, to calculate the coefficients of the details $\alpha_{j,k}$

2 for the reconstruction :

- LoR low-pass filter, to reconstruct the A_j approximation

  high-pass filter HiR, to reconstruct the details D_j

3. Mallat algorithm :DWT-2D with decimation

a) Decomposition

The decomposition procedure according to this algorithm is shown in Figure 1.

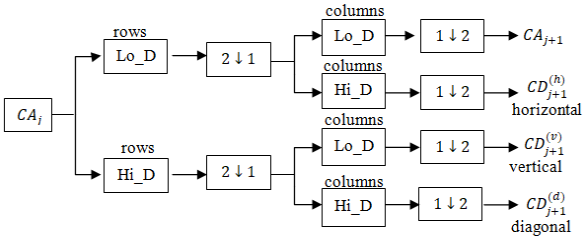

Figure 1. Basic step for DWT-2D decomposition with decimation, where $\mathbf{1}\downarrow\mathbf{2}$ represents the decimation of the rows (preservation of even index rows), and $\mathbf{2}\downarrow\mathbf{1}$ represents the decimation of columns (conservation of even index columns).

b) Reconstruction

The reconstruction of an approximation cA_j (if j=0, A_0 is the final rendered image) from the approximation cA_{j+1} and the set of details at resolution $j+1$, can be summarized in a figure 2.

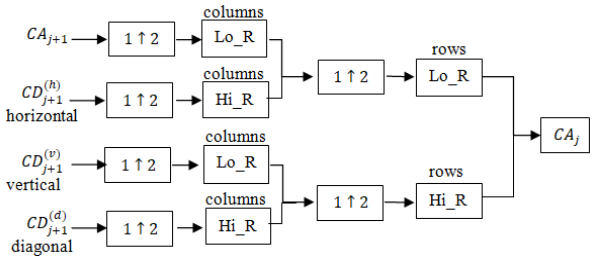

Figure 2. Basic step for DWT-2D reconstruction with decimation

4. Algorithm with holes: DWT-2D without decimation

✓ Decomposition

In the present algorithm, the image is not decimated and keeps its original size. Indeed, at a given resolution j, and to analyze 1 point among the 2^j points, it is the filter that will be oversampled by adding $2^j - 1$ zeros between two coefficients. This addition of zeros is assimilated to an addition of holes, hence the name by hole algorithm.

This algorithm is illustrated in figure 3.

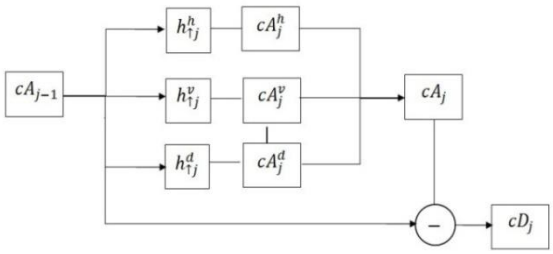

Figure 3. 2D decomposition algorithm without decimation.

✓ Reconstruction

Reconstructing an approximation cA_{j-1} (si j=1, cA_0 is the final rendered image) from the set of approximations cA_j and details at resolution j, this algorithm can be summarized in Figure 4.

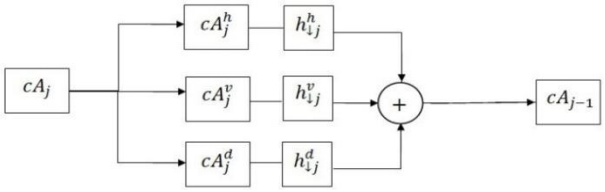

Figure 4. 2D reconstruction algorithm without decimation.

The three convolution results are summed to finally obtain the approximation cA_{j-1} at resolution $j-1$, according to the following equation:

$$\boldsymbol{cA_{j-1}} = \frac{\mathbf{1}}{\mathbf{3}} \sum_{\boldsymbol{p=h,v,d}} \boldsymbol{cA^p_j} * \boldsymbol{h^v_{\downarrow j}} \qquad (8)$$

C. 2D Continuous Wavelet Transform

The 2D continuous wavelet transform (CWT-2D) is done by computing correlation of the 2D signal $f(x,y)$ (such as

an image) with a wavelet $\psi_{a,b,\theta}(x,y)$ that depends not only on the scale parameters a and translations b, but also on a third parameter θ of rotation [4].
It is defined by:

$$\boldsymbol{\psi_{a,b,\theta}(x,y) = \frac{1}{\sqrt{a}}\psi\left(R^{\theta}\left(\frac{x-b}{a},\frac{y-b}{a}\right)\right)} \quad (9)$$

With R^{θ} is a rotation (change of reference frame) matrix:

$$R^{\theta} = \begin{bmatrix}\cos\theta & \sin\theta \\ \sin\theta & -\cos\theta\end{bmatrix}$$

And the calculation of the coefficients $C_f(a,b,\theta)$ of the 2D wavelet transform [4], is done according to:

$$\boldsymbol{C_f(a,b,\theta) = \iint_{-\infty}^{+\infty} f(x,y)\psi^{*}_{a,b,\theta}(x,y)\ dx\,dy} \quad (10)$$

III. The shearlet transform

The Shearlet transform, introduced in 2005 by Labate, Lim et al [5], is like the discrete wavelet transform, it uses a decomposition by means of filters extracted from wavelets and scale function, but unlike it, it is anisotropic, and even better according to [19], it is adapted to the detection of curvilinear shapes, such as retinal vessels, hence our interest in approaching this approach in the segmentation of retinal vessels.

A. The Shearlets

Shearlets as well as discrete wavelets are constructed from generating functions (wavelets) that can be modified with a certain scaling operator, they are scaled anisotropically by means of a shear that orients the wavelet in different orientations [5]. Figure 5 shows the approximation of a curvilinear curve using isotropic bases (wavelets) and anisotropic bases (shearlets). It is clear, that the latter is better suited to approximate curvilinear forms.

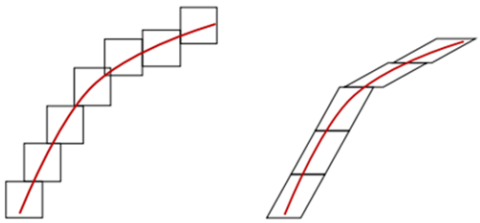

(a) (b)

Figure 5. (a) Approximation of a curve by means of an isotropic basis. (b) Approximation of a curve by means of anisotropic basis [23].

The construction of a Shearlet requires a combination of :

- a scaling operator based on a parabolic scaling matrix $A_a$of the form [6]:

$$\boldsymbol{A_a = \begin{pmatrix} a & 0 \\ 0 & a^{1/2}\end{pmatrix} = \mathbf{diag}\left(\mathbf{a}\ , \mathbf{a^{1/2}}\right);} \quad (11)$$

  Where a is a scaling factor.
- a shear operator, allowing orientation changes. This operator is represented by the shear matrix S_s given by [6]:

$$\boldsymbol{S_s = \begin{pmatrix} 1 & s \\ 0 & 1\end{pmatrix};} \quad (12)$$

Where s is a shear factor.

- a translation factor t to move the shearlet on the 2D plane.

In view of this combination, the shearlet function is expressed as [7]:

$$\boldsymbol{\psi_{a,s,t}(x) = a^{3/4}\psi\left(A_a{}^{-1}S_s{}^{-1}(x-t)\right)} \quad (13)$$

Where $\psi \epsilon L^2(\mathrm{R}^2))$ is a generating function. The shearlets $\psi_{a,s,t}$ would therefore emerge by expansion, shear and translation of the ψ function.

B. Continuous Shearlet Transformation

For a number of scale, shear and translation values, a continuous Shearlet system can be generated by:

$$\boldsymbol{SH_{con}(\psi) = \left\{\psi_{a,s,t}(x) = a^{3/4}\psi\left(A_a{}^{-1}S_s{}^{-1}(x-t)\right) \,/\, a \in R^{+}, s \in R, t \in R^2\right\}} \quad (14)$$

The Shearlet transformation $\mathrm{TSH}_{\psi}(f)$ of a function $f \in L^2(R)$ would be defined by [8]:

$$\boldsymbol{\mathbf{TSH}_{\psi}(f)(\mathbf{a},\mathbf{s},\mathbf{t}) = \iint_{-\infty}^{+\infty} f(x,y)\psi^{*}_{a,s,t}(x,y)dx\,dy} \quad (15)$$

It is used to calculate correlation (degrees of similarity) between the function f and the Shearlet ψ.

C. Discrete Shearlet transformation

A discrete version of the Shearlet system can be obtained by discretizing the set of parameters associated with the continuous Shearlet system, as follows:

$$\begin{cases} \text{the scale factor :} & \mathrm{a} \to 2^{j} \\ \text{the shear factor :} & \mathrm{s} \to k \quad \mathrm{j,k} \in Zet\ \mathrm{m} \in Z^2 \\ \text{the translation parameter :} & \mathrm{t} \to \mathrm{m} \end{cases}$$

Thus, the scale and shear operators become: $A_a \to A_{2j}$ et $S_s \to S_k$

The discrete shearlet system would therefore be [9] :

$$\boldsymbol{SH_{disc}(\psi) = \left\{\psi_{j,k,m}(n) = 2^{3j/4}\psi\left(S_k A_{2j}\,(n-cm)\right)\right\}} \quad (16)$$

where : $\mathrm{n} \in Z^2$ discrete spatial coordinates of the image, and $c \in R_+^2$ is a sampling constant.

Therefore, the calculation of the discrete Shearlet transformation will be as follows:

$$\boldsymbol{TSH_{\psi}(f)(j,k,m) = \iint_{-\infty}^{+\infty} f(x,y)\psi^{*}_{j,k,m}(x,y)dx\,dy} \quad (17)$$
$$\boldsymbol{f \in L^2(R^2)}$$

D. Vascular structure enhancement using the Shearlet transform

The intuitive idea behind this approach is that, since the coefficients of the Shearlet transform are closely related to the curvilinear structures whether major or minor, a complete representation of the retinal vascular tree could be obtained by inverse calculation of the coefficients of the Shearlet transform. This inverse calculation, in this case inversion of equation (3.5), is done as follows [5]:

$$\boldsymbol{f} = \mathbf{TSH}_{\psi}^{-1}\{\mathbf{TSH}_{\psi}\{\boldsymbol{f}\}(\mathbf{a},\mathbf{s},\mathbf{t})\} = \mathbf{TSH}_{\psi}^{-1}\{\langle \boldsymbol{f}, \boldsymbol{\psi}_{a,s,t}\rangle\} = \sum_{\psi \in SH} \langle \boldsymbol{f}, \boldsymbol{\psi}_{a,s,t}\rangle . \boldsymbol{S^{-1}\psi}_{a,s,t} \qquad (18)$$

But as, the number of coefficients of the Shearlet transformation could be important, especially since some coefficients could correspond to slender structures, other than retinal vessels, We will retain only the high coefficients, really representing the curvilinear structures of the vessels, This trimming of the coefficients, will give an enhancement of the curvilinear structures according to the following equation [5]:

$$\boldsymbol{f_n} = \sum_{i \in I} \langle \boldsymbol{f}, \boldsymbol{\psi_i}\rangle . \boldsymbol{S^{-1}\psi_i} \qquad (19)$$

Where I is the set of indices i, associated with the n highest coefficients among the set of all coefficients $\langle f, \psi_{a,s,t}\rangle$.

IV. The DRIVE data base

The Drive image database includes 40 colour fundus images, 7 of which have pathologies. The images are acquired using the fluorescence angiography modality by means of a Canon RC5 with a 45 degree field of view (FOV, Fieled Of View). They are recorded in JPEG format, with a size of 768 * 584 pixels. The image base is divided into two sets, 20 images for training and the rest for testing. It also includes manually segmented images of the vascular network, performed by two experienced ophthalmologists [10].

V. Application on retinal images

step 1. Reading of the image of the bottom of the retina from the DRIVE base. It is a color image of RGB type. (figure 6.a)

step 2. Transformation into a gray level luminance image, or conservation of the green channel only (because it is more contrasted). (figure 6.b)

Figure 6. Image read from the DRIVE database, (a): original image, (b): grayscale image.

step 3. Noise smoothing pre-processing by median filtering of size $[3 \times 3]$. The background of the image becomes more homogeneous and the vessel contours smoother.

step 4. As in the calculation of the various discrete or continuous TO, we proceed to a calculation of convolution with wavelets or filters, to avoid the effect of edge at the level of the disc of the retina, we replace the null values outside the disc of the retina by a value which recalls the contents inside the disc. The choice is carried on the average value of the values inside the disc.

To make this calculation, we need the FOV (Field Of View) mask found in the DRIVE database, and according to the expression :

$$val_{ave} = average(I_{image}(FOV == 255))$$

step 5. Invert the image to make the vessels bright, and the background dark.

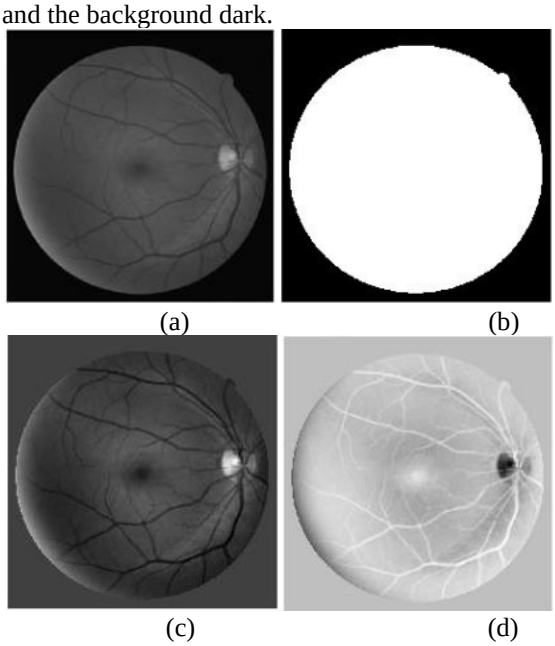

(a) (b) (c) (d)

Figure 7. Preprocessed image, (a): filtered image, (b): the FOV mask, (c): edge effect removal, (d): intensity reversed image.

These 5 steps are common to the algorithms that will be discussed in the following.

A. Application of the Wavelet Transform Algorithm with decimation

For the wavelet transform algorithm with decimation we will use the procedure exposed in section Ⅱ.B.3.

step 6. Creation of the decomposition filters. To do this, we must first choose the appropriate onelette whose shape corresponds to the profile of the blood vessels, in order to better enhance the vascular shapes. The wavelets: 'Daubechies 4 or 5', 'Symplet 6 or 8', 'Coiflet 2 or 3', meet this requirement. In the following we will use the wavelet 'Daubechies 5', shown in figure 8.

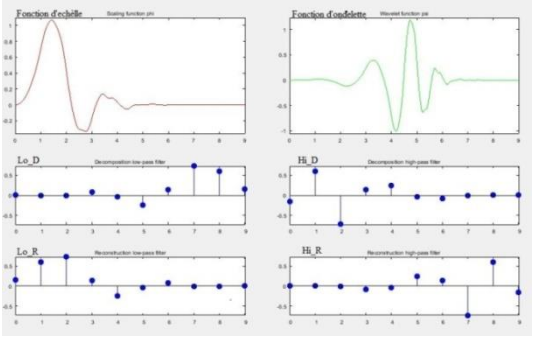

Figure 8. Wavelet 'Daubechies 5', represent the function of Db5 and scale with the 4 associated filters.

step 7. DWT-2D image decomposition with decimation, on 4 levels $(j = 1{:}\,4)$,with the 4 associated filters, according to the procedure explained in section II.B.3, and the results are shown in Figure 9. It is clear that the vessels are enhanced on the detail images.

step 8. To obtain an image where the vessels are enhanced, we will keep only the detail images of levels 2 to 4, because level 1 is too noisy. The sum of all the details at scales 2 to 4, gives us the final image of the enhanced vessels, shown in figure 10.(a).

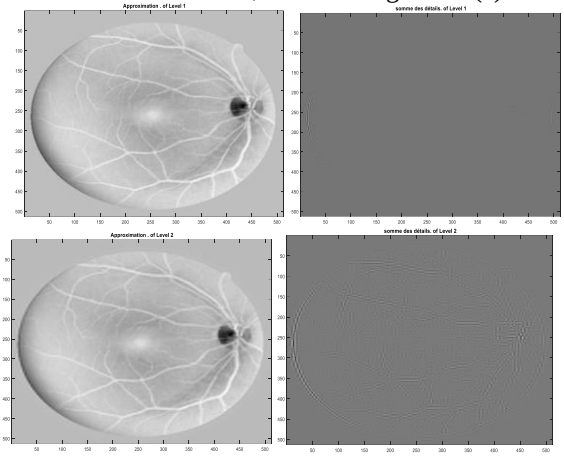

Figure 9.Image decomposed by the wavelet 'Daubichies 5', the left column represents the aproximations and the right column represents the sum of the details (horizontal, vertical and diagonal) for the different scales from 1 to 4.

step 9. Segmentation by the histogram thresholding method, and whose optimal threshold is calculated according to the Otsu method (implemented in Matlab). The result is shown in figure 10.(b).

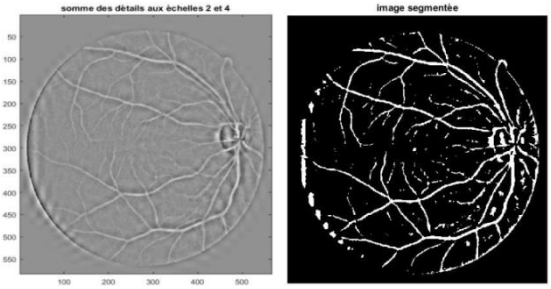

(a) (b)

Figure 10. Image segmentation based on the 2D DWT algorithm.

On the segmented image, we notice that the segmented vessels show discontinuities, and the thin vessels are almost non-existent, this is due to the loss of information during decimation.

B. Application of the Wavelet Transform Algorithm without Decimation

For the wavelet transform algorithm without decimation we will use the procedure outlined in section II.B.4. The algorithm of the transformation without decimation is similar to that of the transform with decimation, the only difference is that at the decomposition we do not decimate the approximation but we oversample the matched filter by inserting zeros.

step 6. The decomposition filters are designed from the filter $h = [1\ 2\ 4\ 6\ 4\ 2\ 1]$, shown in figure 11, the different decomposition filters

$$\boldsymbol{h_{Horizontal} = [1\ 2\ 4\ 6\ 4\ 2\ 1]} \quad (20)$$
$$\boldsymbol{h_{vertical} = transpose(h)} \quad (21)$$
$$\boldsymbol{h_{diagonal} = diag(h)} \quad (22)$$

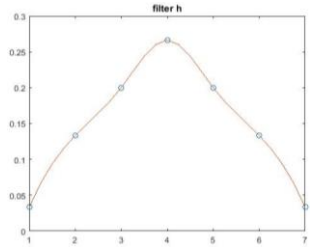

Figure 11. decomposition filter.

step 7. Wavelet decompositions on 4 levels, the horizontal, vertical and diagonal approximations at level j are obtained by convolving the level $j-1$ approximation with the filters above. While the details of level j are obtained by subtracting, from the approximation of level $j-1$, the sum of the resulting approximations of the convolution. At each level $j > 1$ we oversample the 3 filters. Figure 12 shows the results of this step.

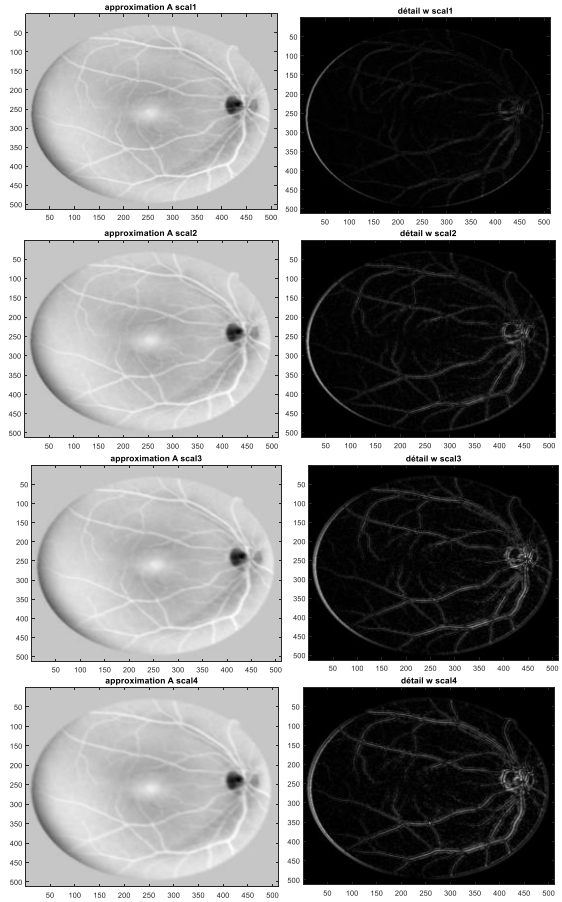

Figure 12. Image decomposed by an h filter, the left column represents the approximations and the right column represents the sum of the details (horizontal, vertical and diagonal) for the different scales from 1 to 4.

step 8. Calculation of the image of the enhanced vessels by summing the details of levels 2 to 4, without level 1 because it is too noisy. Figure 13.(a), shows the result of this step.

step 9. Segmentation by the histogram thresholding method, and whose optimal threshold is calculated according to the Otsu method. The result is shown in figure 13.(b).

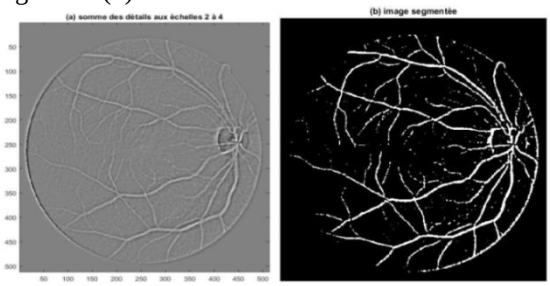

(a) (b)

Figure 13. Image segmentation based on the hole algorithm (a): sum of details at scales 2 to 4, (b): segmented image.

If we compare the results obtained with the 2D DWT algorithm with decimation (figure 10.b) with those obtained with the hole algorithm (figure 13.b), we notice that in the latter there is an appearance of some fine vessels and a decrease in false detections caused by the non-homogeneity of the retina background.

C. Morlet wavelet-based segmentation algorithm

step 6. Generation of the wavelet according to equation (11). The image is correlated with this wavelet, on several scales, and for each scale on several directions, according to equation (3), with b=0 (the calculation is centered on each pixel). Some results of the decomposition are shown in figure 14.

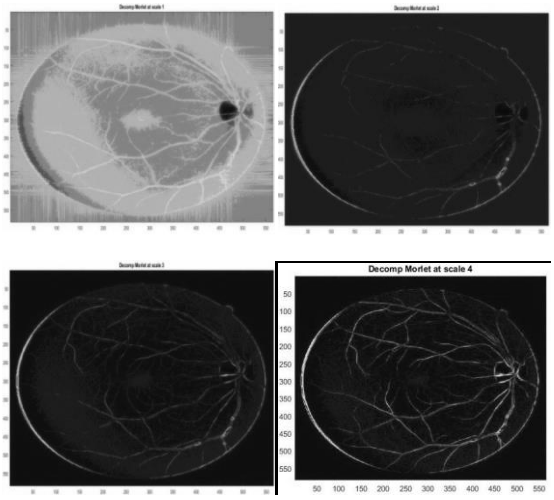

Figure 14. Morlet wavelet decomposition, scale 1 to 4.

step 7. Production of the image where the blood vessels are enhanced.

-On each scale, and for any point of the image, we retain the maximum response on all directions.

$$M_f(a) = \underbrace{\max}_{\theta} C_f(a,\theta)$$

-And for any point in the image, we retain the maximum response on the set of scales. the angle maxima of the coefficients for the different scales and directions.

$$F_f = \underbrace{\max}_{a} M_f(a)$$

The result is shown in Figure 15.a.

step 8. Segmentation by the histogram thresholding method, and whose optimal threshold is calculated according to the Otsu method The result is illustrated in figure 15.b.

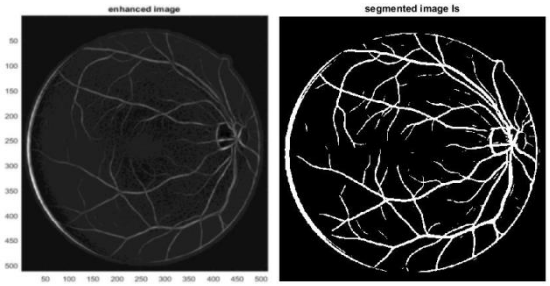

(a) (b)

Figure 15. Morlet wavelet-based image segmentation (a): enhanced image, (b): segmented image

On the segmented image (15.b) we can see a decrease in false detections by comparing the results obtained with the 2D DWT algorithm with decimation (figure 10.b) and those obtained with the hole algorithm (figure 13.b). There is a clear improvement in the segmentation of large vessels and including fine vessels.

D. The segmentation algorithm via the Shearlet Transform

step 3. In the ToolBoxShearlet V3.11, to generate the Shearlet system, the Cohen-Daubechies-Feauven wavelet is used as a generating wavelet. [11]
A 4 scale decomposition was chosen: $a = 2^j\big|_{j=0:3} = [1,2,4,8]$. A shear for k= [1, 1, 3, 3]. (Choice imposed by the ToolBox, due to the fact that the size of the shear vector must be the same as that of the scale vector).

step 4. The decomposition of the image on the shearlet SH_{disc} system, according to equation (18), and then an approximation corresponding to the broadest coefficients is selected according to equation (20). The selection of the wide coefficients is done by thresholding operation. This approximation corresponds to the enhanced image, and is represented in figure 16.b.

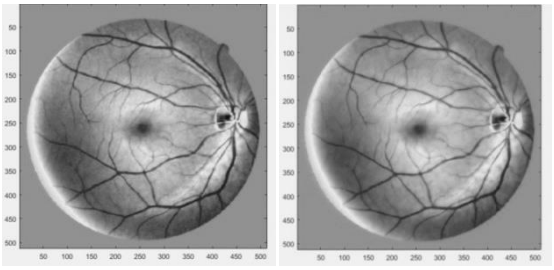

(a) (b)

Figure 16. Image Enhanced retinal image by shearlet decomposition: (a) the original image, (b) the enhanced image.

We notice that in the enhanced image that the vascular structures are more highlighted (enhanced) and have higher intensities than in the original image. In addition, and the background of the retina is completely smoothed.

Segmentation of the enhanced image by thresholding on histogram, as for the segmentation algorithms developed previously. But this time, the CWT-Morlet is applied beforehand to enhance the Gaussian profile of the blood vessel intensity. The results are shown in figure 17.

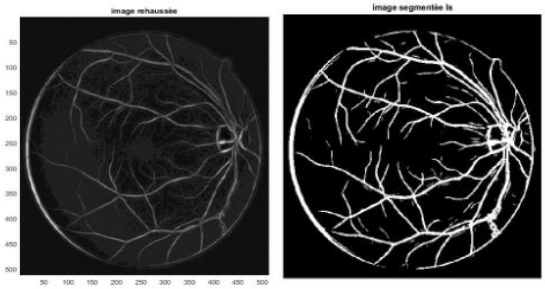

Figure 17. Image segmentation by the shearlet transform: (a) CWT-Morlet enhancement of the image in Figure 3.5.b, (b) segmented image.

We note:

A clear improvement of the segmentation compared to the previous algorithms, because appearance of fine vasculatures absent in the 1st ones. This improvement is due to the basic shape of Shearlet, which by shearing can approximate all curvilinear shapes of any elongation and in any orientation, and thanks to the change of scale, it can approximate vessels of any width.

Also, much less false detections, due to the non-homogeneity of the retinal background. This improvement is due to the approximation enhancement procedure that keeps only the wide coefficients of the Shearlet transformation. Since the geometric structures of the background do not correspond to the elongated shape of the base of the Shearlet. The coefficients of the Shearlet transform related to the background would be small and will be removed in the approximation enhancement procedure.

VI. Performance Measurement

A. Presentation of the performance measures of an algorithm

The performance is evaluated by comparing the image segmented by the algorithm with a reference image, segmented manually by a professional, and contained in the database.

The performance of the algorithm is quantified significantly by :

1. Sensitivity (se):

Indicates the ability of the algorithm to correctly detect retinal vessels, according to the following equation [01]:

$$\boldsymbol{se} = \frac{\boldsymbol{TP}}{\boldsymbol{TP} + \boldsymbol{FN}} \qquad (23)$$

Where TP (true positives): the number of vessel points correctly detected in the retinal images.

And FN (false negatives): the number of points as non-vessels detected.

2. Specificity (sp):

Indicates the ability of the algorithm to distinguish all non-vascular structures, according to the following equation [01]:

$$\boldsymbol{sp} = \frac{\boldsymbol{TN}}{\boldsymbol{TN} + \boldsymbol{FP}} \qquad (24)$$

Where FP (false positives): the number of non-vascular points detected as vessels.

And TN (true negatives): the number of correctly detected non-vessel points.

3. Accuracy (acc):

Measures the ratio of correctly classified pixels (both vessel and non-vessel) to the total number of pixels in the image field of view, according to the following equation [01]:

$$\boldsymbol{acc} = \frac{\boldsymbol{TP} + \boldsymbol{TN}}{\boldsymbol{TP} + \boldsymbol{TN} + \boldsymbol{FP} + \boldsymbol{FN}} \qquad (25)$$

4. La ROC (Receiver Operating Characteristic) :

This is a characteristic curve for the functioning of the receiver, it plots the fraction of the true positive rate (TVP) against the false positive rate (TFP), where :

-The TPV indicates the ratio of the points correctly classified as vessels to the total number of vessel points in the reference image.

$$\boldsymbol{TVP} = \frac{\boldsymbol{TP}}{\textbf{total number of vessel points in the reference image}} \qquad (26)$$

- The TFP indicates the ratio of points incorrectly classified as vessels to the total number of non-vessel points in the reference image.

$$\boldsymbol{TFP} = \frac{\boldsymbol{FP}}{\textbf{total number of non} - \textbf{vessel points in the reference image}} \qquad (27)$$

B. Performance evaluation of the proposed segmentation method

The performance of the proposed retinal vessel segmentation method using the Shearlet transform, after application to all images in the DRIVE database, is shown

in Table 1. In addition, the ROC curve is shown in Figure 19.

Image	Sensitivity	Specificity	Accuracy
01	0,911	0,9039	0,9049
02	0,7989	0,9491	0,9266
03	0,7506	0,936	0,909
04	0,7088	0,9376	0,9071
05	0,7643	0,9544	0,9286
06	0,7113	0,9339	0,9025
07	0,7521	0,9443	0,9189
08	0,6062	0,9542	0,9104
09	0,7946	0,9174	0,903
10	0,7561	0,9606	0,9362
11	0,7133	0,9191	0,8924
12	0,7281	0,941	0,9144
13	0,717	0,9327	0,9021
14	0,8031	0,9388	0,9228
15	0,8019	0,9472	0,9321
16	0,7727	0,9339	0,9128
17	0,7377	0,8988	0,8789
18	0,7565	0,9437	0,9222
19	0,8456	0,9301	0,9199
20	0,8204	0,9141	0,9041
mean	0,7625	0,9345	0,9124

Tableau 1. Performance measures.

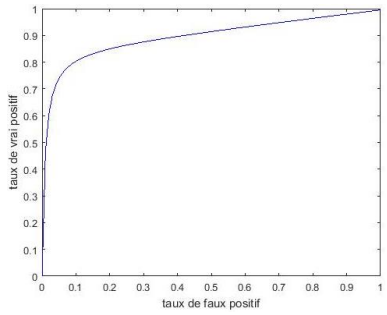

Figure 18. ROC characteristic curve

VII. Conclusion

In the present work we have set ourselves the challenge of developing a method that can segment the retinal vascular tree, taking into account the variability, in terms of size, intensity and orientation of the retinal vessels.

We managed to produce 2 segmentation algorithms based on the discrete wavelet transform with and without decimation, whose results were not up to our expectations, because this transform is anisotropic, and a 3rd algorithm based on the continuous wavelet transform, delivering convincing results but with enough false detections.

We also established a segmentation algorithm based on the Shearlet transform, which allows to enhance the curvilinear structures, such as blood vessels, associated with the continuous wavelet transform by means of the Morlet wavelet to better highlight the gray level profile of the vessels, to finally allow a better segmentation and the results obtained are more than convincing.

In order to compare the last algorithm developed with the retinal vessel segmentation methods cited in the literature, we calculated its performance in terms of sensitivity (0.7625), specificity (0.9345), accuracy (0.9124) and area under the ROC curve (0.8941).

Finally, we recommend, in order to improve the performance of the algorithm and get as close as possible to the expert segmentation, to perform a post-processing on the final image to reduce false detections, to use other segmentation methods, such as the active contour, or to perform a pre-processing to correct the non-homogeneous illumination of the retinal angiography image.

VIII. Bibliographic reference

[1] Chetan L Srinidhi, P Aparna, Jeny Rajan. Recent Advancements in Retinal Vessel Segmentation. DOI 10.1007/s10916-017-0719-2, 2017.

[2] C.Charles, Introduction aux ondelettes. Université de Liège, 2011.

[3] Michel Misiti, Yves Misiti et all, Les ondelettes et leurs application, LAVOISIER, 2003, Paris.

[4] Jo˜ao V. B. Soares, Jorge J. Retinal Vessel Segmentation Using the 2-D Morle.Wavelet and Supervised classification.2006].

[5] *ShearLab 3D. Manual. v1.0. August the 29th, 2013.*

[6] Gitta Kutyniok, Demetrio Labate, Editors, Shearlets Multiscale Analysis for Multivariate Data, Birkhäuser, 2012, Springer New York Dordrecht Heidelberg London.

[7] Kai Hu, Aiguo Song et all, An Image Filter Based on Shearlet Transformation and Particle Swarm Optimization Algorithm, Volume 2015, Article ID 414561, 9 pages.

[8] Sören Häuser, Fast Finite Shearlet Transform: a tutorial, February 8, 2012.

[9] Gitta Kutyniok , Wang-Q Lim, and Gabriele Steidl, Shearlets: Theory and Applications, 2014 WILEY-VCH Verlag GmbH & Co. KGaA,Weinheim.

[10] DRIVE: digital retinal images for vessel extraction, http://www.isi.uu.nl/Research/ Databases/DRIVE , 2004.

[11] www.shearlab.org

[12] Elaheh Imani, Malihe Javidi et all, Improvement of retinal Blood vessel detection using morphological component analysis, 2015 Elsevier Ireland Ltd.